Metabolism Clinical and Experimental 94 (2019) 96–104

Contents lists available at ScienceDirect

Metabolism Clinical and Experimental

journal homepage: www.metabolismjournal.com

A novel GTPCH deficiency mouse model exhibiting tetrahydrobiopterin-related metabolic disturbance and infancy-onset motor impairments

Xiaoling Jiang [a,1], Huazhen Liu [a,1], Yongxian Shao [a], Mingzhi Peng [a], Wen Zhang [a], Duan Li [a], Xiuzhen Li [a], Yanna Cai [a], Ting Tan [b], Xinshuo Lu [a], Jianan Xu [a], Xueying Su [a], Yunting Lin [a], Zongcai Liu [a], Yonglan Huang [c], Chunhua Zeng [a], Ya-ping Tang [b,**], Li Liu [a,*]

[a] Department of Genetics and Endocrine, Guangzhou Women and Children's Medical Center, Guangzhou Medical University, Guangzhou, Guangdong 510623, China
[b] Lab of Neural Development and Behavior Genetics, Institute of Pediatrics, Guangzhou Women and Children's Medical Center, Guangzhou Medical University, Guangzhou, Guangdong 510623, China
[c] Department of Neonatal Screening, Guangzhou Women and Children's Medical Center, Guangzhou Medical University, Guangzhou, Guangdong 510623, China

ARTICLE INFO

Article history:
Received 7 December 2018
Accepted 5 February 2019

Keywords:
GTP cyclohydrolase I deficiency
BH4 deficiency
Dopa-responsive dystonia
GCH1
Mouse model

ABSTRACT

Background: GTP cyclohydrolase I (GTPCH) deficiency could impair the synthesis of tetrahydrobiopterin and causes metabolic diseases involving phenylalanine catabolism, neurotransmitter synthesis, nitric oxide production and so on. Though improvements could be achieved by tetrahydrobiopterin and neurotransmitter precursor levodopa supplementation, residual motor and mental deficits remain in some patients. An appropriate GTPCH deficiency animal model with clinical symptoms, especially the motor impairments, is still not available for mechanism and therapy studies yet.

Objectives and methods: To investigate whether the heterozygous GTPCH missense mutation *p.Leu117Arg* identified from a patient with severe infancy-onset dopa-responsive motor impairments is causative and establish a clinical relevant GTPCH deficiency mouse model, we generated a mouse mutant mimicking this missense mutation using the CRISPR/Cas9 technology. Series of characterization experiments on the heterozygous and homozygous mutants were conducted.

Results: The expressions of GTPCH were not significantly changed in the mutants, but the enzyme activities were impaired in the homozygous mutants. BH4 reduction and phenylalanine accumulation were observed both in the liver and brain of the homozygous mutants. Severer metabolic disturbance occurred in the brain than in the liver. Significant reduction of neurotransmitter dopamine, norepinephrine and serotonin was observed in the brains of homozygous mutants. Live-born homozygous mutants exhibited infancy-onset motor and vocalization deficits similar to the disease symptoms observed in the patient, while no obvious symptoms were observed in the young heterozygous mutant mice. With benserazide-levodopa treatment, survival of the homozygous mutants was improved but not completely rescued.

Conclusions: The GTPCH *p.Leu117Arg* missense mutation is deleterious and could cause tetrahydrobiopterin, phenylalanine and neurotransmitter metabolic disturbances and infancy-onset motor dysfunctions recessively. This is the first GTPCH deficiency mouse model which could be live-born and exhibits significant motor impairments. The different extents of BH4 reduction and phenylalanine accumulation observed between liver and brain in response to GTPCH deficiency gives potential new insights into the vulnerability of brain to GTPCH deficiency.

Abbreviations: AADC, aromatic L-amino acid decarboxylase; AGMO, alkylglycerol mono-oxygenase; BH4, tetrahydrobiopterin; COMT, catechol-*O* methyl transferase; DA, dopamine; DBH, dopamine β-hydroxylase; DOPAC, dihydroxyphenylacetic acid; DRD, dopa-responsive dystonia; E, epinephrine; GCH1, GTP cyclohydrolase I (gene); GTPCH, GTP cyclohydrolase I (protein); HVA, homovanillic acid; KI, knock-in; KO, knock-out; MAO, monoamine oxidase; NE, norepinephrine; NO, nitric oxide; NOS, nitric oxide synthases; PAH, phenylalanine hydroxylase; PNMT, phenylethanolamine-*n*-methyl transferase; PTPS, 6-pyruvoyltetrahydropterin synthase; SPR, sepiapterin reductase; TH, tyrosine hydroxylase; TPH, tryptophan hydroxylases; USV, ultrasonic vocalization; 3-MT, 3-methoxytyramine; 5-HIAA, 5-hydroxyindoleacetic acid; 5-HT, serotonin.

* Correspondence to: L. Liu, Department of Genetics and Endocrine, Guangzhou Women and Children's Medical Center, Guangzhou Medical University, Guangzhou, Guangdong 510623, China.
** Correspondence to: Y.-p. Tang, Lab of Neural Development and Behavior Genetics, Institute of Pediatrics, Guangzhou Women and Children's Medical Center, Guangzhou Medical University, Guangzhou, Guangdong, 510623, China.
E-mail addresses: yptang12@yahoo.com (Y. Tang), liliuchina@qq.com, liliuxia2013@gmail.com (L. Liu).
[1] The first two authors contributed equally to this work.

https://doi.org/10.1016/j.metabol.2019.02.001
0026-0495/

1. Introduction

GTP cyclohydrolase I (GTPCH), encoding by gene *GCH1*, is the rate-limiting enzyme in the synthesis of tetrahydrobiopterin (BH4) [1]. BH4 is the critical co-factor for enzyme phenylalanine hydroxylase (PAH), tyrosine hydroxylase (TH), tryptophan hydroxylases (TPHs), nitric oxide synthases (NOSs) and alkylglycerol mono-oxygenase (AGMO) [2] (Fig. 1). GTPCH deficiency therefore could affect phenylalanine catabolism, synthesis of neurotransmitters dopamine (DA), norepinephrine (NE), epinephrine (E) and serotonin (5-HT), production of nitric oxide, and metabolism of ether lipids [3].

Because of the neurotransmitter metabolic deficits, patients with GTPCH deficiency typically develop dopa-responsive dystonia (DRD). This disease could either be inherited dominantly with incomplete penetrance (Segawa's disease) or be inherited recessively [4]. Generally, the dominant cases are mild and late-onset, while the recessive cases are severe and early-onset. Previously, we identified a novel *GCH1* missense mutation: *p.Leu117Arg* (NP_000152.1) in a patient with an intermediate phenotype [5]. The proband's mother and grandfather also carried this missense mutation but exhibited normal. As we were unable to identify the other potential deleterious mutation in the proband's *GCH1* gene, whether this mutation was a dominant causative mutation with incomplete penetrance, or it might be recessive and compound with other unknown functional intronic mutation for example, still need validation.

Residual motor dysfunction and mental retardation still existed in our patient after benserazide-levodopa treatment. This might be caused by delayed diagnosis and treatments. However, it has been reported that even with early treatments of L-DOPA and BH4, not all patients achieved normal neurocognitive development [6,7]. The disease progress of GTPCH deficiency is still largely unknown. Improved therapy for this genetic metabolic disorder is urgently needed. An animal model which could well mimic the clinical symptoms will be useful for the mechanism study and therapy development.

There were two mouse models with *Gch1* mutations reported previously. The *hph-1* hyperphenylalaninemic mouse, generated by *N*-ethyl-*N*-nitrosourea mutagenesis, had reduced *Gch1* expression and showed moderate systemic BH4 deficiency [8]. Though the *hph-1* mouse had been considered as a model of dominantly inherited GTPCH deficiency, it did not exhibit any motor impairment like the human [9]. On the other hand, *Gch1* knock-out (KO) mouse, which was reported by Douglas and his colleagues recently [10], showed embryonic lethality around E11.5 to E13.5. Even rescuing with supplementation of L-DOPA and sepiapterin, no live pups could be born. Thus the postnatal disease process of GTPCH deficiency could not be investigated.

In this study, we established a novel *Gch1* 'knock-in' (KI) mouse model carrying the *p.Leu117Arg* mutation using the CRISPR/Cas9 technology. Half of the homozygous KI mice ($Gch1^{KI/KI}$) could be live-born. The live-born $Gch1^{KI/KI}$ pups were visibly normal on the day of birth, but similar to the patient, significant growth retardation, motor and vocalization dysfunctions were observed soon after then. To the best of our knowledge, this *Gch1* KI mouse model is the first live-born GTPCH deficiency mouse model with significant motor and vocalization dysfunctions.

2. Material and methods

2.1. Animals

All mice were housed at a SPF animal facility with a 12-hour-light/dark schedule. Food and water were accessed ad libitum. For tissue

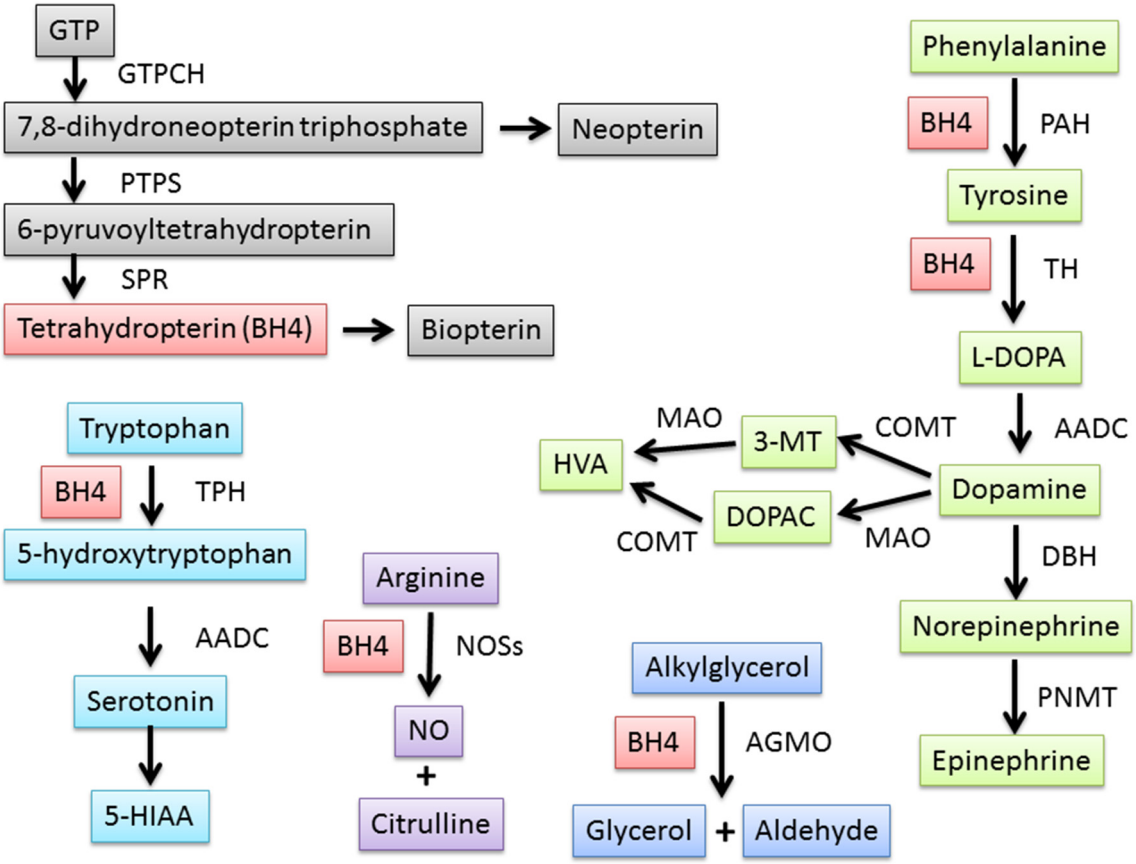

Fig. 1. The metabolic pathways which could be affected by GTPCH deficiency. GTPCH is the rate-limiting enzyme in the synthesis of BH4. BH4 is the critical co-factor for enzyme PAH, TH, TPHs, NOSs and AGMO. GTPCH deficiency could therefore affect phenylalanine catabolism, synthesis of neurotransmitters dopamine, norepinephrine, epinephrine and serotonin, production of NO, and metabolism of ether lipids. PTPS, 6-pyruvoyltetrahydropterin synthase; SPR, sepiapterin reductase; AADC, aromatic L-amino acid decarboxylase; DBH, dopamine β-hydroxylase; PNMT, phenylethanolamine-*n*-methyl transferase; COMT, catechol-O methyl transferase; MAO, Monoamine oxidase; 3-MT, 3-methoxytyramine; DOPAC, dihydroxyphenylacetic acid; HVA, homovanillic acid; 5-HIAA, 5-hydroxyindoleacetic acid; NO, nitric oxide.

collection, the pups were fast decapitated, and the tissues were isolated and frozen in liquid nitrogen immediately. All the procedures performed were approved by the Animal Care and Use Committee of Guangzhou Medical University.

2.2. Generation of a mouse model to mimic the patient GTPCH p.Leu117Arg mutation

Human GTPCH *p.Leu117* is conserved to mouse GTPCH *p.Leu108* (Fig. 2A). The Cas9 mRNA, sgRNA and oligo donor with the desired mutation were co-injected into fertilized C57BL/6 eggs (Fig. 2B). The sgRNA used was CATCAAATATAGCATCATTCAGG, and the following oligo donor was used as the homology-directed repair template: AAAATATTTACTAT CCTTCAGT ATTTAACCAATTTTGTGTTTTCCCGGTTCCAGATGT**ACG**GAATG ATGCTATATTTGATGAAGATCATGACGAGATGGTGATTGTGAAGGACATA GATAT. The *p.Leu108Arg* mutation (CTG to CGG) was introduced into the oligo donor together with a silent mutation (GTC to GTA) to prevent the binding of sgRNA to the oligo donor. Founders with the expected mutation were identified by sequencing the PCR amplicons of tail DNA. The mutant mice were crossed to C57BL/6 for at least three generations before used in the intercross of $Gch1^{KI/+} \times Gch1^{KI/+}$ to eliminate potential off-targeting mutations. Potential off-targeting sites were predicted using CCTOP (https://crispr.cos.uni-heidelberg.de/) and examined by direct sequencing (Supplemental File). The whole *Gch1* coding region and flanking sequences were also sequenced. No off-targeting events were detected in the mice examined.

A PCR-RFLP based genotyping method was developed to facilitate the genotyping procedure (Fig. 2C), which was based on the recognition of the silent mutation by restriction enzyme *CviQI* (New England Biolabs, USA). The following primers were used for the genotyping PCR reaction: mGch1-KI-F: GGAAGTGTGATTGTGGGAAGA and mGch1-KI-R: CAAATGGAACAAGG TGATGCT.

2.3. Quantitative reverse transcriptase PCR

Total RNA was isolated from the liver or brain using TRIzol Reagent™ (Invitrogen, USA). cDNA was synthesized from two μg of total RNA using

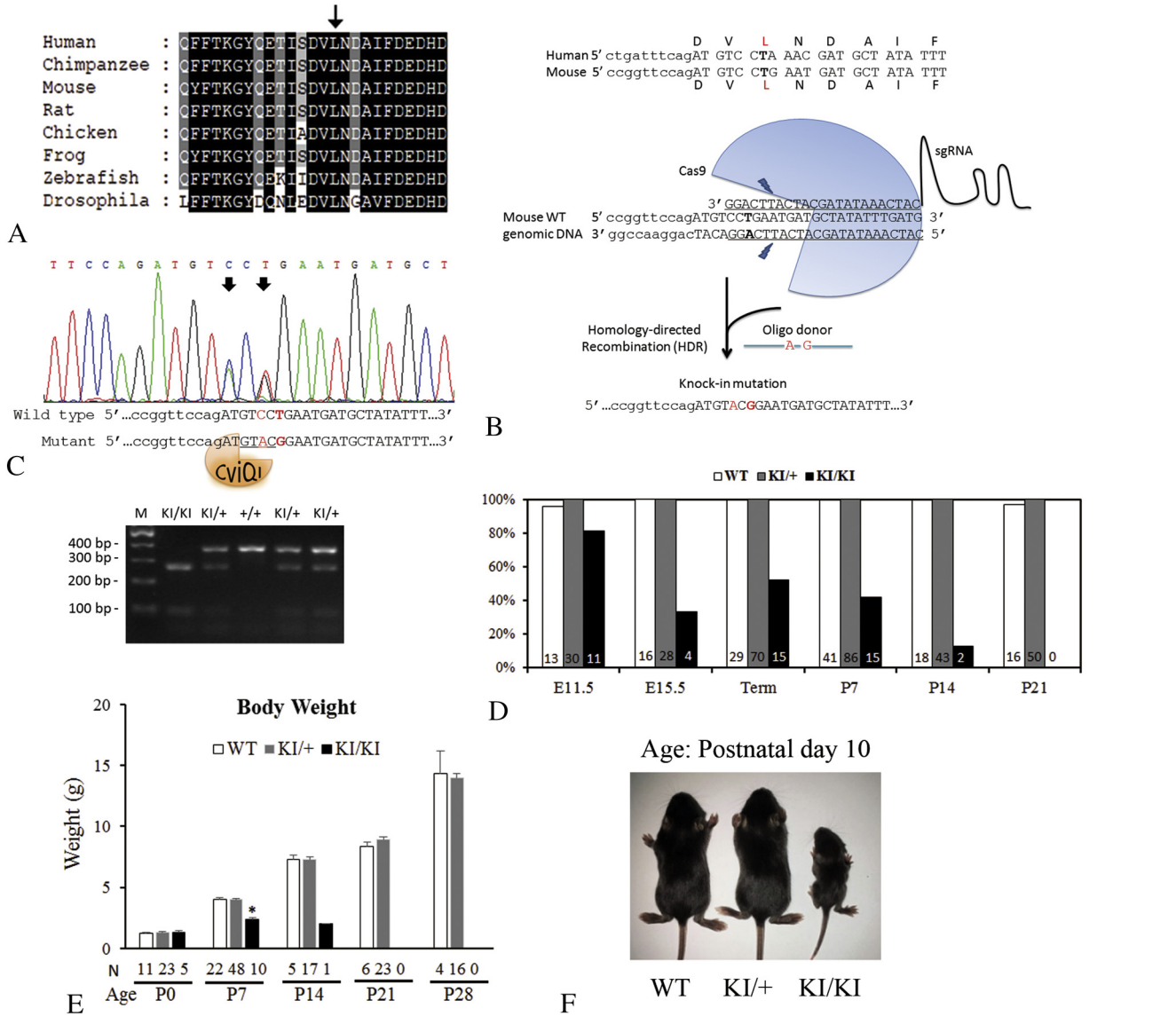

Fig. 2. Generation of a *Gch1* knock-in mouse model with patient-derived missense mutation. (A) Conservation of the *GCH1* gene. Human *GCH1 p.Leu117* is conserved to mouse *Gch1 p.Leu108*. (B) Schematic showing the generation of *Gch1 p.Leu108Arg* knock-in mouse model using the CRISPR/Cas9 system. A silent mutation (GTC to GTA) was also introduced into the oligo donor with the *p.Leu108Arg* mutation (CTG to CGG) to prevent the binding of sgRNA to the oligo donor. (C) A PCR-RFLP based genotyping method was developed to facilitate the genotyping of the mutants. The 366 bp PCR product from the mutant allele could be digested by restriction enzyme *CviQI* to 269 bp and 97 bp. (D) Frequency of progeny of each genotype from the $Gch1^{KI/+} \times Gch1^{KI/+}$ intercross to the expected Mendel's ratio. The numbers of pups observed were noted inside the bars. (E) Postnatal growth of the live-born $Gch1^{KI/KI}$ pups. N, number of pups measured. (F) A picture of the pups from a same litter on P10.

PrimeScript™ RT Master Mix kit (TAKARA, Japan). Real-time quantitative PCR was performed on the CFX96™ Real-Time PCR systems (Bio-RAD) using SYBR® Premix Ex Taq™ II (TAKARA, Japan). The following mouse *Gch1* specific primers were used: *mGch1*-RT-F: cgccatgcagtacttcacca and *mGch1*-RT-R: tgaggcgctcttgaacttgt. Triplicate reactions for each sample were conducted. *Gapdh* had been used as the internal reference gene.

2.4. Western blot

Western blot analysis was conducted using mouse GTPCH antibody (1:500, sc-271482, Santa Cruz, USA). β-actin (1:1500, sc-47778, Santa Cruz, USA) was used as the reference. The densities of the bands were quantified with software Image J, and the GTPCH expression level was normalized to the internal β-actin.

2.5. Ex-vivo GTPCH activity test

The GTPCH activity was assessed following the method described by Bonafe and her colleagues [11] with some modification. Briefly, about 20 mg liver tissue was homogenized in 700 μL homogenization buffer [11] by sonication (Sonics VCX130, USA) in ice bath. The mixture was then centrifuged at 15,000 rpm for 5 min. The supernatant was desalted using the prepacked His Spin Trap column (GE Healthcare, UK) and Zeba™ spin desalting column (Thermo Scientific, USA). 50 μL of the filtrate was mixed with 150 μL reaction solution [11] which containing 2.67 mmol/L GTP. The GTPCH catalysis reaction was carried out at 37 °C for 60 min. The catalytical product dihydroneopterin triphosphate was then oxidized and dephosphorylated to neopterin following Bonafe's protocol [11]. The final product was filtered through 0.22 μm membrane, and analyzed by HPLC (Shimadzu Prominence Chromatograph System, Japan). All the chemicals used were purchased from Sigma-Aldrich (Merck, Germany) or Guangzhou Chemical Reagent Factory (China). Both empty samples without liver extract and liver samples without the one hour catalytic incubations were used as blanks. D-(+)-Neopterin (Sigma-Aldrich, N3386) was used as standard analyte. Protein concentrations of the liver lysates were measured using the Pierce™ BCA protein assay kit (Thermo Scientific, USA) and used for normalization of the GTPCH activities.

2.6. BH4 quantifications

Quantifications of BH4 were conducted following Kaneko's protocol with some modification [12]. Briefly, about 30 mg liver or half of the brain was homogenized in 500 μL extraction buffer [12] by sonication (Sonics VCX130, USA) in ice bath. 200 μL of the supernatant was equally separated into two 1.5 mL eppendorf tubes, followed by addition of 100 μL of 0.2 N HCl or 0.2 M NaOH, respectively. Differential oxidization process was initiated by the addition of acidic or alkaline iodine solution [12], respectively. After 1 h incubation in the dark at room temperature, the oxidization process was quenched by addition of 2% (*w*/*v*) ascorbic acid. The chemicals and solutions used were purchased from Sigma-Aldrich (Merck, Germany) or Guangzhou Chemical Reagent Factory (China). The samples were filtered through 0.22 μm membrane before loading on the autosampler of HPLC system (Shimadzu Prominence chromatograph system, Japan). 6-Biopterin (Sigma-Aldrich, B2517) was used as standard analyte. BH4 derived biopterin was calculated according to Kaneko's protocol [12]. Protein concentrations were measured using the Pierce™ BCA protein assay kit (Thermo Scientific, USA) and used for normalization.

2.7. Tissue amino acid analysis

For amino acid quantification, 100 μL of the tissue homogenate supernatant from above BH4 quantification was used. 100 μL of perchloric acid solution (0.6 mol/L) was added to the supernatant, and the mixture was vortexed for 5 min followed by centrifugation at 13,000 rpm for 15 min. The supernatant was then filtered through a 0.22 μm membrane and injected into the HPLC system (Agilent 1200 series, USA) for automation pre-column derivatization and data acquisition as described previously [13]. Tissue weight was used for normalization.

2.8. Brain monoamines

The brain monoamines were measured by liquid chromatography-tandem mass spectrometry (LC-MS/MS). Briefly, half of the brain was homogenized and sonicated in 800 μL of ice-cold methanol-acetonitrile (1:1, containing 0.1% ascorbic acid and 2% formic acid). Samples were then centrifuged at 4 °C to remove proteins. 500 μL of the supernatant was evaporated to dryness under vacuum for monamines analysis. The dried supernatant was re-dissolved in 100 μL of water and derivatized by propyl chloroformate. Derivatives were extracted by ethylacetate and analyzed by LC-MS/MS. Analytes included DA, dihydroxyphenylacetic acid (DOPAC), 3-methoxytyramine (3-MT), homovanillic acid (HVA), NE, 5-HT, 5-hydroxyindoleacetic acid (5-HIAA). All the standards were purchased from Sigma-Aldrich. Brain weight was used for normalization.

2.9. Immunohistochemistry

For immunohistochemistry, the brains of pups were dissected out after fast decapitation and fixed in 4% paraformaldehyde for at least 24 h at 4 °C. The fixed brains were then embedded in paraffin. Coronal sections of 5 μm were prepared. Antigen was retrieved by heating in the citrate buffer (G1202, Servicebio, China). Immunohistology was performed by incubation the sections with primary antibody TH (1:500, ab112, Abcam, UK) and HRP-conjugated IgG secondary antibody (1:200, GB23303, Servicebio, China), then visualized using the DAB Kit (G1211, Servicebio, China). The nuclei were counter stained with hematoxylin.

2.10. Assessment of the motor functions

Righting reflex and hindlimb suspension tests were performed on postnatal day 7 (P7) according to Feather-Schussler and Ferguson's protocol [14]. A maximum of 2 min was given for each trial and all tests were repeated in triplicate. Forelimb grip strengths of four-week-old mice were measured using the Animal Grip Strength Test Meter (IITC Life Science Inc., USA). Each mouse was repeated to the test five times.

2.11. Ultrasonic vocalization (USV)

For USV recording, pups were taken individually from the mother and placed in a small container with fresh bedding. USVs were recorded in a home-made sound-proof foam box for 5 min using the UltraSoundGate condenser microphone (CM16, Avisoft Bioacoustics, Germany) and Avisoft RECORDER software (version 4.2.27, Avisoft Bioacoustics, Germany) with the sampling rate of 250 kHz in 16-bit format. Fast Fourier transforms were conducted at 512 FFT length, 100% frame, Hamming window, and 75% time window overlap. An automated threshold-based algorithm with 5 ms hold time was used to detect USVs. The call numbers and average call durations were analyzed.

2.12. Benserazide-Levodopa treatment

Dissolved Madopar® Tablet (Roche, Switzerland) in the water was utilized as levodopa supplementary. Oral administration of 16.9 μg/g benserazide-levodopa/body weights (i.e. 13.5 μg/g L-Dopa and 3.4 μg/g benserazide) by a micropipette was started from P2 twice a day.

2.13. Statistics

The data was presented in the format of means ± standard errors. The ANOVA test was conducted to evaluate the differences in samples. *Post hoc* Dunnet test comparing the mutants with WT controls were performed when a p-value <0.05 was suggested.

3. Results

3.1. Generation of a novel Gch1 knock-in mouse model with a missense mutation

Human *GCH1 p.Leu117* is conserved to mouse *Gch1 p.Leu108*. We employed CRISPR/Cas9 technology to generate a mouse mutant with exact *Gch1 p.Leu108Arg* mutation (*NM_008102.3:c.323 T > G*). The $Gch1^{KI/+}$ mice were viable and fertile, and no apparent motor impairments were observed. Inter-cross of $Gch1^{KI/+} \times Gch1^{KI/+}$ were set up to obtain $Gch1^{KI/KI}$. As shown in Fig. 2D, the birth ratio of $Gch1^{KI/KI}$ was only half of the expected Mendel's ratio. Time mating experiments indicated that the utero death of $Gch1^{KI/KI}$ embryos mainly occurred between E11.5 to E15.5. The live-born $Gch1^{KI/KI}$ pups were visibly normal at the day of birth. However, growth retardation and poor weight gain were observed then after (Fig. 2E). The body weight of $Gch1^{KI/KI}$ was significantly lower than the wild-type (WT) and heterozygous $Gch1^{KI/+}$ measured on P7. None of the $Gch1^{KI/KI}$ pups could survive more than two weeks.

3.2. Activity of the mutant GTPCH protein in the liver

Gch1 is most abundantly expressed in the liver. Quantitative PCR demonstrated that the expression levels of liver *Gch1* mRNA were not significantly changed in the mutants (Fig. 3A). Further assessment of the GTPCH protein in the liver also revealed no difference between WT and the mutants (Fig. 3B). The ex-vivo GTPCH activity test, which was based on the quantification of 7,8-dihydroneopterin catalyzed from the substrate GTP, showed that samples from $Gch1^{KI/KI}$ exhibited lower enzyme activities (Fig. 3C). In-silico analysis of the human mutant GTPCH protein suggested that the missense mutation located at the entrance of the GTP-binding pocket (Fig. 3D). Arginine is positively charged and has a longer side chain than leucine. The substitution of argine for leucine may interfere the entry of GTP into its binding pocket.

GTPCH deficiency mainly affects the biosynthesis of BH4. Measurement of the liver BH4 revealed decreased BH4 in the mutant pups (Fig. 3E). As BH4 is the critical cofactor of PAH which converts phenylalanine to tyrosine, we also measured the amino acids in the liver. Significant accumulation of phenylalanine was observed in the $Gch1^{KI/KI}$ liver (Fig. 3F).

3.3. Abnormal levels of BH4, amino acid and neurotransmitters in the $Gch1^{KI/KI}$ brain

The expression of *Gch1* was also not significantly changed in the brain of mutant pups (Fig. 4A), while BH4 was significantly decreased (Fig. 4B) and phenylalanine was significantly accumulated (Fig. 4C) in the brain of $Gch1^{KI/KI}$. The reduction of BH4 and accumulation of phenylalanine in $Gch1^{KI/KI}$ were severer in the brain than those in the liver.

As BH4 deficiency could affect the synthesis of neurotransmitter DA, NE, and 5-HT (Fig. 1), we assessed whether levels of brain neurotransmitters were changed in $Gch1^{KI/KI}$. Measurement of monoamines in the brain of P7 pup revealed that neurotransmitter DA was significantly reduced in $Gch1^{KI/KI}$ compared to that in WT (5% of WT level, Fig. 4D). DA metabolites (DOPAC, 3-MT and HVA) were also significantly reduced (data not shown). Turnover rate of DOPAC/DA was found significantly reduced in $Gch1^{KI/KI}$ (Fig. 4E) which may be caused by the compensatory effect of low DA level. NE was also found significantly reduced in $Gch1^{KI/KI}$ (7% of WT level, Fig. 4F). In contrast, the NE/DA turnover rate was increased in $Gch1^{KI/KI}$ (Fig. 4G). Further, 5-HT was also significantly reduced in $Gch1^{KI/KI}$ brain than that in WT (Fig. 4H).

3.4. TH was undetectable in the $Gch1^{KI/KI}$ striatum

TH is the rate-limiting enzyme of DA synthesis. It had been demonstrated that, unlike the other BH4-dependent enzymes, the stability of TH protein was specifically sensitive to BH4 level, especially at the

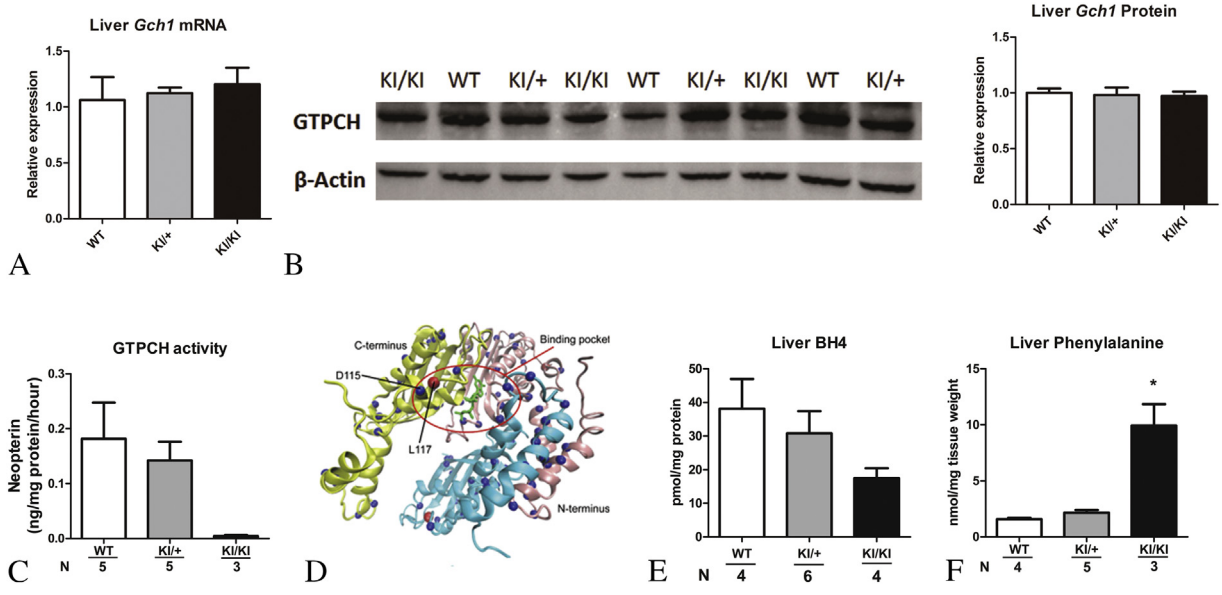

Fig. 3. Effects of the missense mutation on the activities of GTPCH in the liver. (A) Expression of *Gch1* mRNA in the liver did not significantly changed ($N = 3$–4 per genotype group, $p > 0.05$). (B) Expression of the GTPCH protein in the liver did not show difference. (C) Ex-vivo GTPCH activity test indicated decreased enzyme activity in $Gch1^{KI/KI}$. (D) In-silico analysis of the *p.Leu117Arg* missense mutation in the human GTPCH decamer complex suggested that *Leu117* (highlighted with red ball) was locating at the entrance of the GTP binding pocket. Substitution of arginine for leucine could interfere the entry of GTP into its binding pocket. (E) Decreased BH4 level was observed in the $Gch1^{KI/KI}$ liver. (F) Liver phenylalanine was significantly elevated in the $Gch1^{KI/KI}$ comparing to that in the WT ($p < 0.05$). N, Number of animals tested. All the liver samples used were collected from pups of age P7.

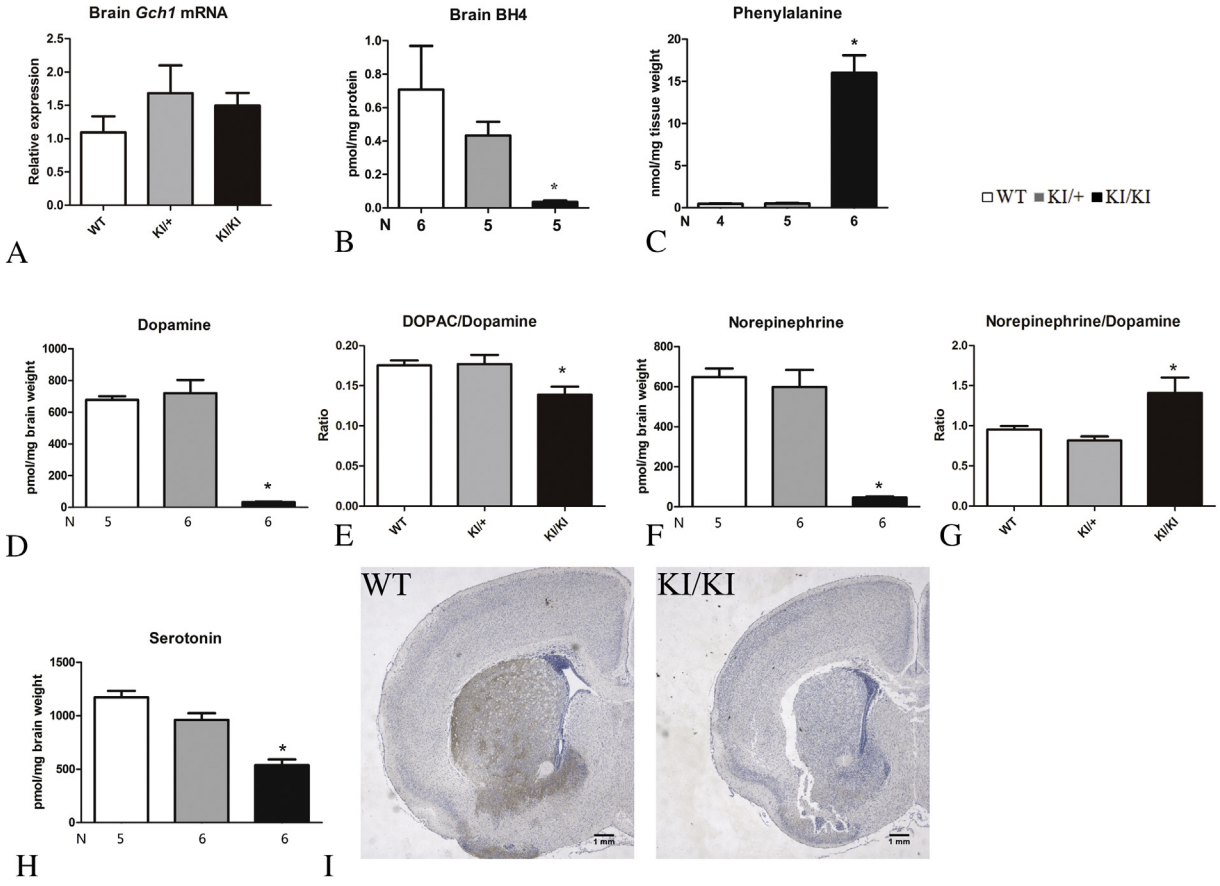

Fig. 4. Abnormal neurotransmitter metabolism observed in the *Gch1*$^{KI/KI}$ brain. (A) Expression of *Gch1* in the brain was not significantly changed (N = 3–5 per genotype, $p > 0.05$). (B) BH4 was significantly decreased in the *Gch1*$^{KI/KI}$ brain comparing to WT ($p < 0.05$). (C) Phenylalanine was significantly accumulated in the *Gch1*$^{KI/KI}$ brain. (D) Dopamine was significantly reduced in the brain of *Gch1*$^{KI/KI}$. (E) The turnover rate of DOPAC/DA was also significantly reduced in *Gch1*$^{KI/KI}$. (F) Norepinephrine was significantly reduced in *Gch1*$^{KI/KI}$. (G) Turnover rate of NE/DA was significantly increased in *Gch1*$^{KI/KI}$. (H) 5-HT was significantly decreased in the *Gch1*$^{KI/KI}$ brain. N, Number of animals tested. *$p < 0.05$, comparing to WT. (I) Immunohistological staining for TH in the WT and *Gch1*$^{KI/KI}$ striatum. Scale bars = 1 mm. TH staining was absence in the *Gch1*$^{KI/KI}$ striatum (right). All the brain samples analyzed were isolated from pups of age P7.

dopaminergic neuronal nerve fibers [15]. The striatum is rich with dopaminergic neuronal nerve fibers. We assessed TH protein levels in the *Gch1*$^{KI/KI}$ striatum by immunohistology. The results showed that TH was undetectable in the *Gch1*$^{KI/KI}$ striatum (Fig. 4I).

3.5. Motor and vocalization deficits observed in *Gch1*$^{KI/KI}$

The *Gch1*$^{KI/KI}$ pups were hypoactive and exhibited abnormal walking posture. Hindlimb clasping was observed when hung a *Gch1*$^{KI/KI}$ pup by its tail (Fig. 5A). In the righting reflex test performed on P7, *Gch1*$^{KI/KI}$ need more time to return to the prone position (Fig. 5B). In the hindlimb suspension test, *Gch1*$^{KI/KI}$ pups also performed worse and fell earlier than the WT and *Gch1*$^{KI/+}$ pups (Fig. 5C–E). These observations indicated that sever motor dysfunctions existed in *Gch1*$^{KI/KI}$. As language developmental delay was observed in the patient, we tried to measure the oral communication of the pups by utilizing the separation-induced USV test [16]. Comparing to WT and heterozygous pups, *Gch1*$^{KI/KI}$ called significantly less (Fig. 5F). The average duration per call was also significantly shorter (Fig. 5G). In contrast, *Gch1*$^{KI/+}$ performed similarly to their WT littermates. Further, no difference was observed between *Gch1*$^{KI/+}$ and WT in the forelimb grip strength measured on 4-weeks-old (Fig. 5H).

3.6. Benserazide-levodopa treatment extended the lifespan of *Gch1*$^{KI/KI}$

GTPCH deficiency is “dopa-responsive” in clinical. Initially, we tried to rescue the *Gch1*$^{KI/KI}$ pups by supplementing 1 mg/mL of L-DOPA in the drinking water of the dams but failed to observe any improvements. Then we tried to treat the pups with a high dose of benserazide-levodopa administrated twice a day starting from P2. This treatment improved the survival of *Gch1*$^{KI/KI}$ pups up to one month, though the growth retardation was still significant and the postnatal death could not be completely rescued (Fig. 6).

4. Discussion

Both incomplete dominant and recessive GTPCH deficiencies have been reported [4]. Autosomal dominant GTPCH deficiency is the most common type of DRD [17], while the recessive form is relatively rare but more severe and complex. We recently identified a novel *GCH1 p.Leu117Arg* missense mutation in a patient with infancy-onset dopa-responsive motor dysfunctions [5]. As only one allele was mutated in this proband, and her mother and grandfather also carried this missense mutation but exhibited normal, whether the *GCH1 p.Leu117Arg* was the causative mutation remained controversial.

In this study, we generated a mouse mutant carrying the *GCH1 p.Leu117Arg* missense mutation (corresponding to *Gch1 p.Leu108Arg* in mice). The heterozygous KI mice (*Gch1*$^{KI/+}$) grew normally and showed no difference with their wild-type (*Gch1*$^{+/+}$) littermates in the forelimb grip strength test performed on four-weeks-old. In contrast, significant motor dysfunctions, growth retardation, and lethality were observed in the homozygous *Gch1*$^{KI/KI}$ pups. Levels of BH4 and neurotransmitters DA, NE and 5-HT were also found dramatically decreased in the *Gch1*$^{KI/KI}$ brain. In accordance with the observations in the other two

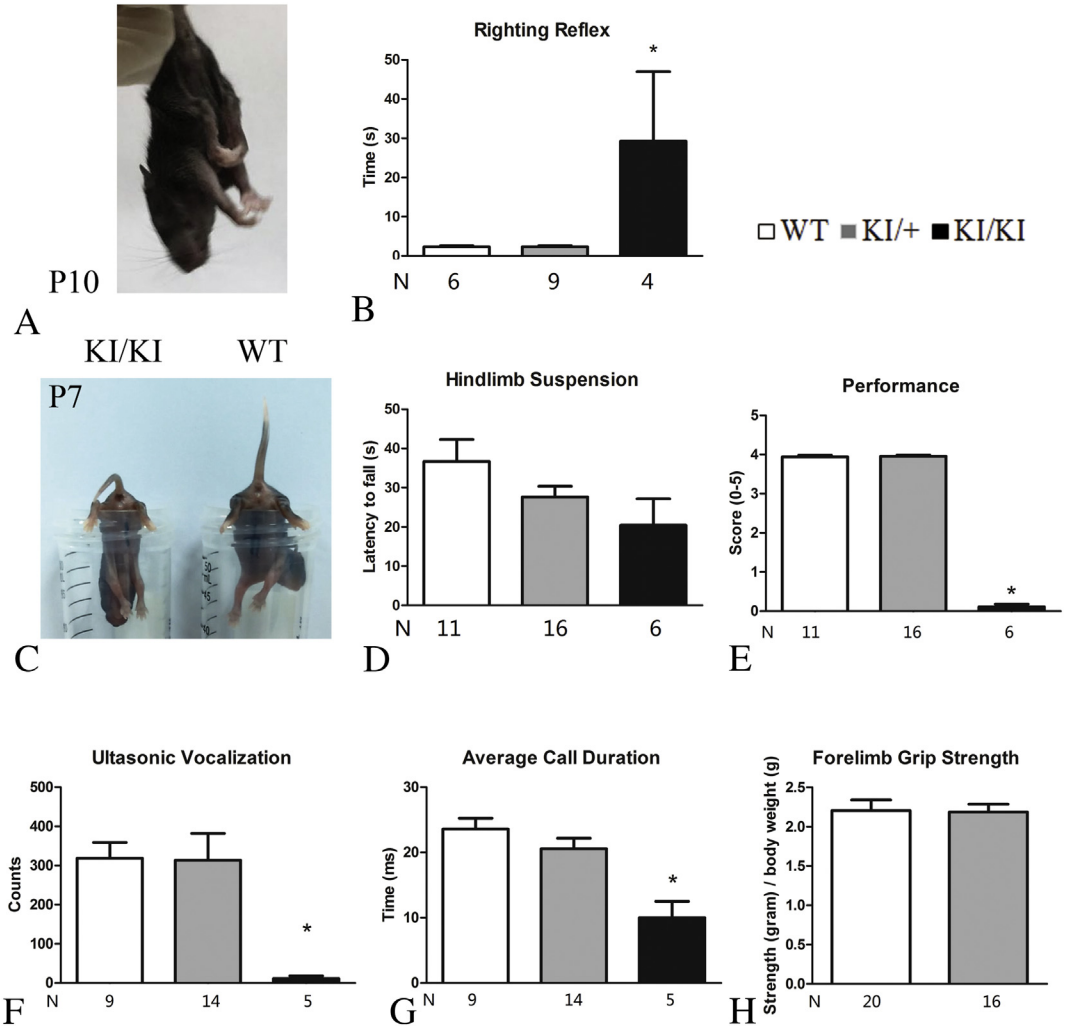

Fig. 5. *Gch1*$^{KI/KI}$ pups displayed motor and vocalization impairments. (A) Picture showing the hindlimb clasping observed in *Gch1*$^{KI/KI}$ pups on P10. (B) Righting reflex tests performed on P7. *Gch1*$^{KI/KI}$ pups need more time to return to the prone position. (C–E) In the hindlimb suspension tests performed on P7, *Gch1*$^{KI/KI}$ pups were unable to hold their tails straight. The *Gch1*$^{KI/KI}$ pups fell earlier and performed worse than their littermates. (F–G) The *Gch1*$^{KI/KI}$ pups called significantly less and shorter than their littermates in the separation induced USV test performed on P7. (H) The heterozygous *Gch1*$^{KI/+}$ performed similar to their WT littermates in the forelimb grip strength test performed at 4-weeks-old. N, Number of animals tested. *$p < 0.05$, comparing to WT.

BH4 deficiency mouse models, *Ptps* (6-pyruvoyl-tetrahydropterin synthase) KO mouse and *Spr* (sepiapterin reductase) KO mouse [15,18], TH, the rate-limiting enzyme of DA synthesis was undetectable in the *Gch1*$^{KI/KI}$ striatum. All these observations suggested that the human GTPCH *p.Leu117Arg* mutation is deleterious and likely to be a recessive mutation. Another undetected deleterious recessive mutation compound with the GTPCH *p.Leu117Arg* might exist in the patient.

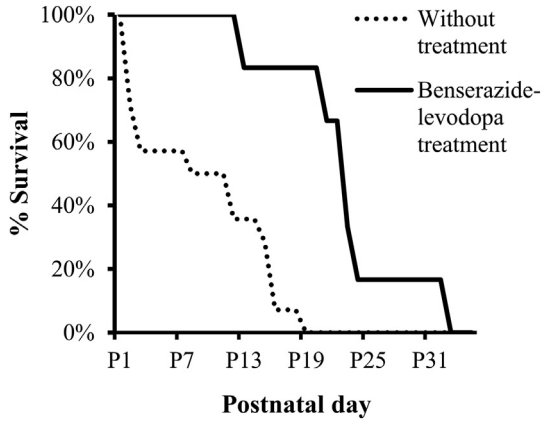

Fig. 6. Benserazide-Levodopa treatment. Survival of *Gch1*$^{KI/KI}$ pups with Benserazide-Levodopa treatment started on P2 twice a day ($N = 6$), comparing to those without treatment ($N = 14$).

There were two *Gch1* mouse mutants reported previously, but either no signs of motor impairments were observed [9] or no alive pups could be born [10]. It is indeed difficult to create animal models with neurotransmitter deficiencies. As shown in the creating of an AADC (aromatic L-amino acid decarboxylase, involving DA and 5-HT synthesis) deficiency animal model [19], a slight increase of *Aadc* mRNA level erased all the disease symptoms observed in an *Aadc* splicing error KI mouse model, while completely knock-out of the *Aadc* resulted in embryonic lethal [20]. As the best of our knowledge, the *Gch1* KI mouse model reported in this study was the first live-born *GCH1* deficiency mouse model with significant motor and vocalization deficits.

GTPCH is the first and rate-limiting enzyme in the common de novo BH4 synthesis pathway. In this study, we observed that the degree of BH4 reduction in the brain and liver was different in *Gch1*$^{KI/KI}$. BH4 of *Gch1*$^{KI/KI}$ was reduced to 5.04% of WT in the brain but was only reduced to 45.81% of WT in the liver. A difference in the BH4 reduction in the brain and liver was also observed in the SPR deficiency mice [15]. However, in contrary to our observation in the GTPCH deficiency, more reduction of BH4 in the liver (1.1% of WT) than in the brain (40.5% of

WT) was reported in the SPR deficiency mouse model. Our observation highlights the specific vulnerable of brain to the *GCH1*-mutation caused BH4 deficiency. Multiple alternate de novo and salvage pathways have been reported in addition to the common de novo BH4 synthesis pathway [1]. The difference of BH4 reduction in the brain and liver suggested that different alternate BH4 biosynthesis pathways were used in the two organs. Examination of the expression of the enzymes and metabolites in these alternate and salvage pathways may elucidate the differential regulation of BH4 synthesis in response to GTPCH/BH4 deficiency in the brain and liver. It is known that transportation of the oral supplemented BH4 through the blood-brain barrier and plasma membrane is not efficient [21,22]. Studies on the regulation of BH4 synthesis pathways may be helpful for the development of alternate therapies.

BH4 is the essential cofactor of PAH, which is responsible for the converting of phenylalanine to tyrosine. Hyperphenylalaninemia (HPA) and phenylketonuria (PKU) were frequently observed in patients with BH4 deficiency because of the impaired function of PAH [6]. HPA would cause oxidative stress to the neurons and decreasing the brain antioxidant defense [23], which finally results in mental retardation and progressive motor disorders [24]. However, in contrast with DRD, HPA and PKU were not always observed in the *GCH1*-mutation caused BH4 deficiencies [4]. The specific higher accumulation of phenylalanine in the brain than liver (35 fold compared to 6 fold increment) observed in our $Gch1^{KI/KI}$ mouse model suggested that potential brain damage caused by phenylalanine accumulation may also contribute to the disease phenotype even though HPA or PKU was not observed in some *GCH1*-mutation caused BH4 deficiency patients.

Oral administration of benserazide-levodopa twice a day extended the survival of $Gch1^{KI/KI}$ pups as illustrated in Fig. 6. The response of the $Gch1^{KI/KI}$ pups to the benserazide-levodopa treatment confirmed the "dopa-responsive" feature of the GTPCH deficiency disorder. DA is a well-known neurotransmitter modulating voluntary motor behaviors and motor functions [25]. It also affects normal feeding [26] and growth-hormone release [27]. DA was dramatically reduced to as less as 5% of WT in the $Gch1^{KI/KI}$ brain. Role of DA deficiency in the growth retardation and lethality of $Gch1^{KI/KI}$ pups is explicit. However, the BH4 deficiency also affects the function of TPHs and NOSs. TPHs are the rate-limiting enzymes of 5-HT synthesis. 5-HT plays important roles both in the central and peripheral nervous system. Growth retardation and postnatal deaths were also observed in half of the *Tph2* KO mice [28]. 5-HT in $Gch1^{KI/KI}$ brain was reduced to half of the normal level. Whether this magnitude of reduction of 5-HT would have effects on an individual's survival still need further investigation. Defects in NOSs enzymes could cause deficits in multiple systems, including the cardiovascular disease [29]. However, considering that NOSs have higher affinities with BH4 [30], and residual GTPCH activity and BH4 still existed in the $Gch1^{KI/KI}$, deleterious effects caused by NOSs deficiency may be minimal. Additional BH4 and/or 5-HT supplementation [31] or transfer to a more permissive genetic background [32] might be able to further improve the survival of $Gch1^{KI/KI}$ pups.

Expression levels of the mutant *Gch1* mRNA and protein were unchanged in the $Gch1^{KI/KI}$ pups comparing to those in their littermates. Ex-vivo enzyme activity assay showed that mutant GTPCH enzyme activity was reduced to 2.44% of the WT in the liver. These observations indicated that GTPCH deficiency in $Gch1^{KI/KI}$ was caused by the impaired function of the mutant protein, not potential degradation or down-regulation of the mutant protein. In-silico analysis suggested that the *p.Leu117Arg* missense mutation may block the entry of substrate GTP to its binding pocket in the GTPCH complex (Fig. 3D).

As no apparent abnormal motor impairments were observed in the heterozygous pups, how could a heterozygous mutation in the patient cause such severe motor symptoms remains a question. Studies on the patient-derived induced pluripotent stem cells (iPSC) may be able to give insights into the genetic factors interacting with the GTPCH *p.Leu117Arg* missense mutation.

5. Conclusions

In this study we confirmed that the GPTCH *p.Leu117Arg* missense mutation is a deleterious recessive mutation, and generated the first GPTCH deficiency mouse model with infancy-onset motor and vocalization impairments, which well modeling the clinical manifestation of the recessive form of human GTPCH deficiency. Benserazide-levodopa treatment could partly rescue the postnatal lethality of the $Gch1^{KI/KI}$ pups. The severer BH4 reduction and phenylalanine accumulation observed in the brain of $Gch1^{KI/KI}$ pups highlighted the vulnerable of brain to *GCH1*-mutation caused BH4 deficiency. This novel *Gch1* KI mouse model will be fascinating for the mechanism and therapy study of the human metabolic disease GTPCH deficiency.

Acknowledgment

We would like to acknowledge the help from the staff of Clinical Laboratory of Endocrine, Guangzhou Women and Children's Medical Center, the staff of the Core Facility of Guangzhou Institute of Pediatrics, and Dr. Lili Ge for her help in the animal genotyping.

Funding

This study was supported by the National Natural Science Foundation of China: 81671119 to L.L. and 81600986 to X.J.; supported by the Municipal Healthcare Joint-Innovation Major Project of Guangzhou: 201604020020 to L.L.; supported by the Guangzhou Municipal Science and Technology Project: 201804010079 to X.J.

Conflict-of-interest/financial disclosure statement

None of the authors declare conflict of interest.

Author contributions

L.L., YP.T. and X.J. conceived and organized this study. L.L., W.Z., D.L., X.L., Y.L.,Y.H. and C.Z. participated in the diagnosis and treatment of the patient. X.J. initiated the generation of the mutant mouse model, and supervised the mice breeding and behavior tests, while H.L., T.T. and J.X. executed them. Y.S. performed the in-silico analysis of the mutant protein. H.L. and Y.S. measured the GTPCH enzyme activity. H.L. and M.P. measured the neurotransmitters and BH4. H.L. and Y.C. measured the tissue amino acids. H.L. X.L. and Z.L. performed the RT-PCR and Western blot. X.J. and X.S. performed the immunohistology. H.L. and X.J. performed the drug treatment experiment. X.J. and H.L. analyzed the data. X.J. wrote the draft, L.L. and YP.T. revised the paper. All the authors have read and approved the final article.

Appendix A. Supplementary data

Supplementary data to this article can be found online at https://doi.org/10.1016/j.metabol.2019.02.001.

References

[1] Kapatos G. The neurobiology of tetrahydrobiopterin biosynthesis: a model for regulation of GTP cyclohydrolase I gene transcription within nigrostriatal dopamine neurons. IUBMB Life 2013;65:323–33.
[2] Werner ER, Blau N, Thöny B. Tetrahydrobiopterin: biochemistry and pathophysiology. Biochem J 2011;438:397–414.
[3] Watschinger K, Werner ER. Alkylglycerol monooxygenase. IUBMB Life 2013;65:366–72.
[4] Wijemanne S, Jankovic J. Dopa-responsive dystonia-clinical and genetic heterogeneity. Nat Rev Neurol 2015;11:414–24.
[5] Zhang W, Zhou Z, Zhen L, et al. Dopa-responsive dystonia in Chinese patients: including a novel heterozygous mutation in the GCH1 gene with an intermediate phenotype and one case of prenatal diagnosis. Neurosci Lett 2017;644:48–54.

[6] Opladen T, Hoffmann G, Blau N. An international survey of patients with tetrahydrobiopterin deficiencies presenting with hyperphenylalaninaemia. J Inherit Metab Dis 2012;35:963–73.
[7] Ponzone A, Blau N, Guardamagna O, et al. Progression of 6-pyruvoyl-tetrahydropterin synthase deficiency from a peripheral into a central phenotype. J Inherit Metab Dis 1990;13:298–300.
[8] Hyland K, Gunasekara RS, Munk-Martin TL, et al. The hph-1 mouse: a model for dominantly inherited GTP-cyclohydrolase deficiency. Ann Neurol 2003;54:S46–8.
[9] Nasser A, Bjerrum OJ, Anne-Marie H, et al. Impaired behavioural pain responses in hph-1 mice with inherited deficiency in GTP cyclohydrolase 1 in models of inflammatory pain. Mol Pain 2013;9:1–14.
[10] Douglas G, Hale AB, Crabtree MJ, et al. A requirement for Gch1 and tetrahydrobiopterin in embryonic development. Dev Biol 2015;399:129–38.
[11] Bonafé L, Thöny B, Leimbacher W, et al. Diagnosis of dopa-responsive dystonia and other tetrahydrobiopterin disorders by the study of biopterin metabolism in fibroblasts. Clin Chem 2001;47:477–85.
[12] Kaneko YS, Mori K, Nakashima A, et al. Determination of tetrahydrobiopterin in murine locus coeruleus by HPLC with fluorescence detection. Brain Res Protocol 2001;8:25–31.
[13] Yi P, Liu L, Mei H, et al. Establishment of reference range of plasma amino acids for younger Chinese children by reverse phase HPLC. J Pediatr Endocrinol Metab 2011;24:733–8.
[14] Feather-Schussler DN, Ferguson TS. A battery of motor tests in a neonatal mouse model of cerebral palsy. J Vis Exp 2016(117):e53569.
[15] Yang S, Lee Y, Kim J, et al. A murine model for human sepiapterin-reductase deficiency. Am J Hum Genet 2006;78:575–87.
[16] Hammerschmidt K, Fischer J. Ultrasonic vocalizations in mouse models for speech and socio-cognitive disorders: insights into the evolution of vocal communication. Genes Brain Behav 2011;10:17–27.
[17] Clot F, Grabli D, Cazeneuve C, et al. Exhaustive analysis of BH4 and dopamine biosynthesis genes in patients with Dopa-responsive dystonia. Brain 2009;132:1753–63.
[18] Sumi-Ichinose C, Urano F, Kuroda R, et al. Catecholamines and serotonin are differently regulated by tetrahydrobiopterin. A study from 6-pyruvoyltetrahydropterin synthase knockout mice. J Biol Chem 2001;276:41150–4116.
[19] Lee NC, Shieh YD, Chien YH, et al. Regulation of the dopaminergic system in a murine model of aromatic L-amino acid decarboxylase deficiency. Neurobiol Dis 2013;52:177–90.
[20] Hwu WL, Lee NC, Chien YH, et al. AADC deficiency: occurring in humans, modeled in rodents. Adv Pharmacol 2013;68:273–84.
[21] Longo N. Disorders of biopterin metabolism. J Inherit Metab Dis 2009;32:333–42.
[22] Ishikawa T, Imamura K, Kondo T, et al. Genetic and pharmacological correction of aberrant dopamine synthesis using patient iPSCs with BH4 metabolism disorders. Hum Mol Genet 2016;25:5188–97.
[23] Wajner M, Latini A, Wyse AT, et al. The role of oxidative damage in the neuropathology of organic acidurias: insights from animal studies. J Inherit Metab Dis 2004;27:427–48.
[24] Embury JE, Charron CE, Martynyuk A, et al. PKU is a reversible neurodegenerative process within the nigrostriatum that begins as early as 4 weeks of age in Pah (enu2) mice. Brain Res 2007;1127:136–50.
[25] Vitrac C, Benoit-Marand M. Monoaminergic modulation of motor cortex function. Front Neural Circuits 2017;11:72.
[26] Szczypka MS, Rainey M, Kim DS, et al. Feeding behavior in doopamine-deficient mice. PNAS 1999;96:11214–2138.
[27] Diaz-Torga G, Feierstein C, Libertun C, et al. Disruption of the D2 doopamine receptor alters GH and IGF-I secretion and causes dwarfism in male mice. Endocrinology 2002;143:1270–9.
[28] Alenina N, Kikic D, Todiras M, et al. Growth retardation and altered autonomic control in mice lacking brain serotonin. PNAS 2009;106:10332–1033.
[29] Mungrue IN, Bredt DS, Stewart DJ, et al. From molecules to mammals: what's NOS got to do with it? Acta Physiol Scand 2003;179:123–35.
[30] Pastor CM, Williams D, Yoneyama T, et al. Competition for tetrahydrobiopterin between phenylalanine hydroxylase and nitric oxide synthase in rat liver. J Biol Chem 1996;271:22538–4534.
[31] Elzaouk L, Leimbacher W, Turri M, et al. Dwarfism and low insulin-like growth factor-1 due to dopamine depletion in $Pts^{-/-}$ mice rescued by feeding neurotransmitter precursors and H_4-biopterin. J Biol Chem 2003;278:28303–11.
[32] Tanabe LM, Martin C, Dauer WT. Genetic background modulates the phenotype of a mouse model of DYT1 dystonia. PLoS One 2012;7:e32245.